CHEST INJURIES AND INJURY MECHANISMS IN OBLIQUE LATERAL IMPACTS

Narayan Yoganandan, Frank A. Pintar, Thomas A. Gennarelli
Department of Neurosurgery
Medical College of Wisconsin
VA Medical Center
Milwaukee, WI USA

Peter G. Martin, Stephen A. Ridella
US Department of Transportation
NHTSA, Washington, DC USA

ABSTRACT

A majority of laboratory-driven side impact injury assessments are made using post mortem human subject (PMHS) under the pure 90-degree lateral mode. Because real-world injuries occur under pure and oblique modes, this study was designed to evaluate injury metrics and injury mechanisms with PMHS under the latter vector. Anthropometrical data were obtained and functional x-rays were taken. Specimens were seated on a sled and lateral impact acceleration was applied such that the load vector was at an angle of 20- or 30-degrees. The study determined forces in the thorax, abdomen and pelvis; deflection profiles at the levels of the axilla and mid-sternum representing the thorax, and at the tenth rib level representing the abdomen; and accelerations at the upper and lower dorsal spine and pelvis. These response data are valuable in oblique lateral impact assessments.

Key Words: biomechanics, injuries, side impacts, thorax, full scale tests

INJURIES DUE TO SIDE IMPACTS can be classified as stemming from pure lateral, i.e., 90-degree or from oblique load vectors. The United States Department of Transportation side impact crashworthiness tests include impacting a stationary vehicle on the driver side with a 1,360 kg moving deformable barrier. The barrier impacts the vehicle at an angle of 27 degrees. The impact velocity of the barrier for the Federal motor vehicle safety standard 214 compliance tests, is 54 km/h, and for the consumer-aiding New Car Assessment Program (NCAP) test it is 62 km/h (CFR 2000). Depending on the mass of the vehicle, the resulting change in velocity can range from 24 to 32 km/h. The event attempts to mimic intersection impacts. Similar energies are incorporated in Standards from other countries and other evaluations although differences exist in terms of the impacting vector and mass. The European regulations ECE-95 specify pure lateral, that is, 90-degree impact from a 950 kg "mobile" deformable barrier at a velocity of 50 km/h (ECE-95 1995). The side impact test configuration from the Insurance Institute for Highway Safety in the United States is a 50 km/h perpendicular impact into the driver side of a passenger vehicle. The moving deformable barrier that strikes the test vehicle weighs 1,500 kg, and it has a front-end shaped to simulate the typical front end of a pickup or sports utility vehicle.

A recent field study shows that conditions such as intrusion and an obliquely directed impact vector may be more detrimental to occupant safety (Pintar et al. 2007). An analysis of 49 cases using

the Crash Injury Research and Engineering Network, CIREN, database, revealed that oblique impact has characteristic injury patterns and the analysis hypothesized injury mechanisms associated with this vector (Pintar et al. 2007). Almost all laboratory-driven side impact injury assessments using intact PMHS have been done under the pure lateral mode, and hence, injury mechanisms and injury metrics are derived for this mode. Similar studies are lacking for oblique impact. Because real world injuries also occur under oblique modes, the objective of the present study was to determine biomechanical metrics such as forces, accelerations, and deflections, and chest injuries associated with this impact vector.

METHODS

Unembalmed PMHS were procured, and medical records were evaluated and screened for HIV, and Hepatitis A, B, and C. Anthropomorphic data and pretest x-rays were obtained according established procedures (Pintar et al. 1997). Specimens were dressed in tight-fitting leotards, and a mask covered the head/face. Prepared subjects were placed on a Teflon-coated bench seat, 1.3 meter in length, fixed to the platform of a deceleration sled, configured with an impacting load wall. Four plates (upper plate for measuring contact forces with the mid-thorax, middle plate for the abdomen, lower plate for the pelvis, and extremity plate for the lower extremities) were used in the load wall design. The configuration of the load wall was such that, to simulate an oblique side impact, the abdominal and thoracic plates of the load wall were angled 20 or 30 degrees. Figure 1 shows the schematic of the load wall and sled buck. Figure 2 shows a frontal schematic of the obliqueness of the load wall design. PMHS pressurization was done according established protocol (Pintar et al. 1997; Yoganandan et al. 2004). The test matrix included experimentation with two specimens under each oblique load vector.

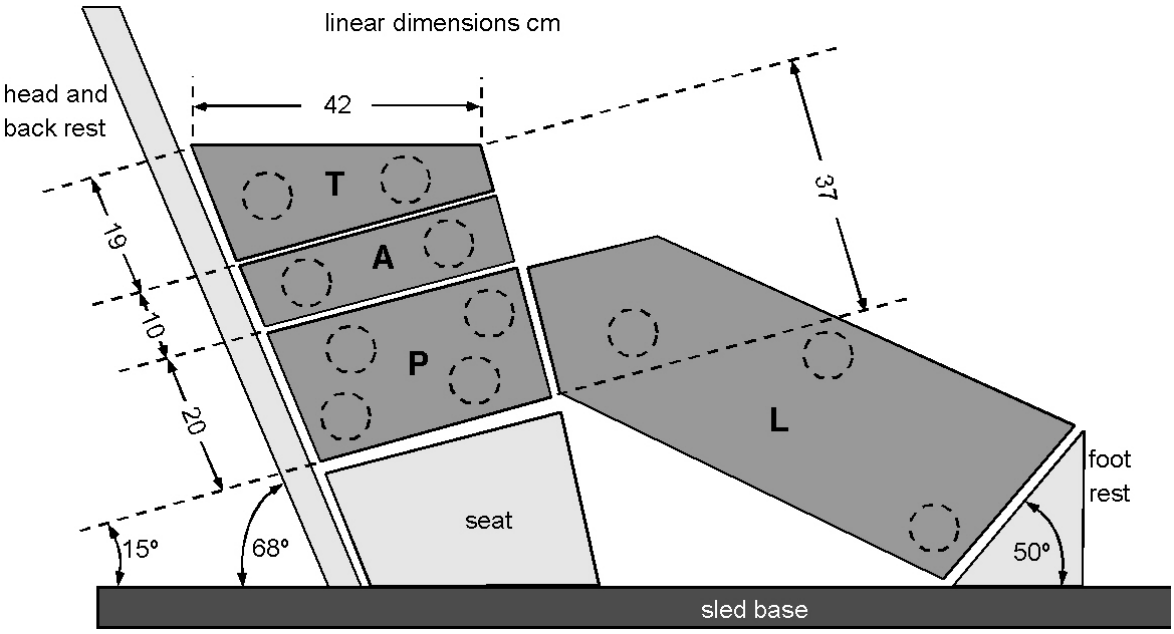

Figure 1: Schematic of the side impact buck with the thoracic (T), abdominal (A), pelvis (P), and extremity (L) plates to measure impact forces. Load cells are shown as dotted circles in the illustration. As can be seen, multiple load cells were used to gather biomechanical data.

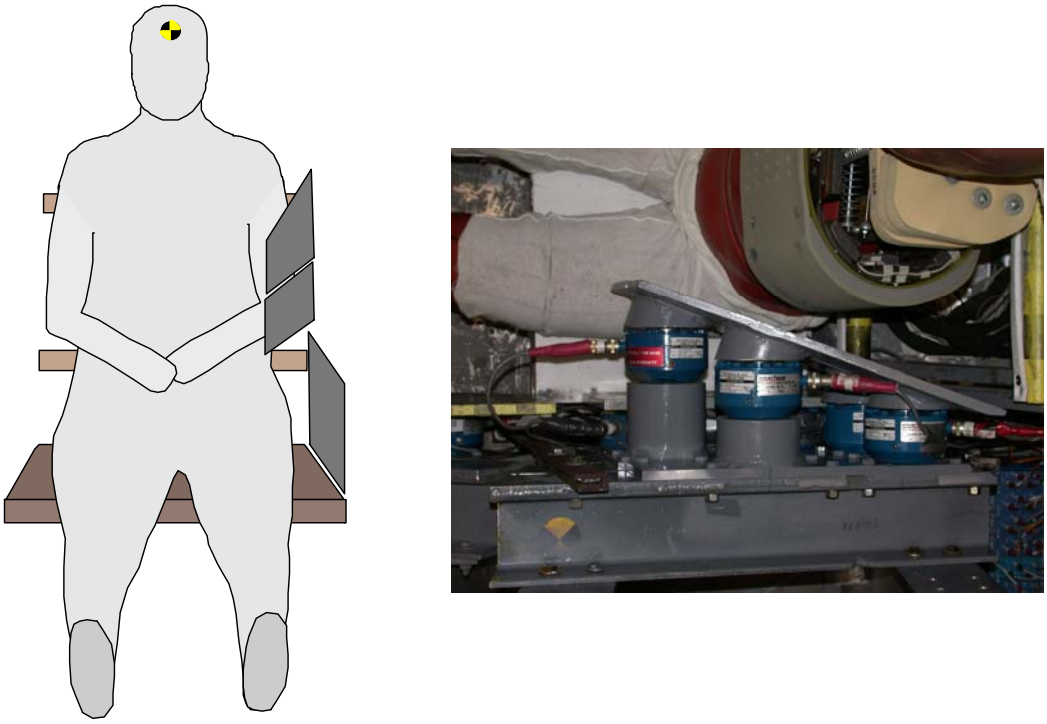

Figure 2: Schematic of the obliquity of the thoracic and abdominal plates of the load wall along with the normally seated occupant used in the test setup for imparting lateral left side acceleration. Left side shows the frontal view and right side shows the top view of the setup.

The following instrumentation was used to gather data. An accelerometer on the sled was used to obtain the change in velocity. A pyramid-shaped nine-accelerometer package (PNAP) was fixed to the head (Yoganandan et al. 2006). The 3-2-2-2 design of PNAP consisted of three sets of biaxial accelerometers (Entran model EGE-73B, Fairfield, NJ) mounted to the triangular base of the pyramid and one triaxial accelerometer mounted at its vertex. The three base arrays constituted the three biaxial components, and the vertex contained the triaxial component. Positions and orientations of all accelerometers were determined using a three-dimensional coordinate measuring device. In addition, tri-axial accelerometers were fixed to the upper and lower thoracic spinous processes, T1 and T12 levels, and sacrum. Eleven load cells, two each in the thorax and abdomen, four in the pelvis, and three in the extremity, were used to record the dynamic forces. Furthermore, three chestbands were fixed at the level of the axilla (upper), xyphoid process (middle), and tenth rib (lower) to measure deformation-time (contours) histories during impact. The chestband provided time-history signals of each strain gage at every 80 microseconds. Using the software provided by NHTSA, chest deformation contours were computed at every millisecond. The computation assumed no change in the circumference of the band at any time interval. The contours were calculated by setting the two reference points on the closest gauges aligned to the midsagittal plane of the spine. Deflections were computed by finding the maximum change in length between a gauge on the struck side of the specimen and a point located at a fixed distance from the spine along a vector between the gauges most closely aligned with the spine and sternum. The fixed distance was set to one-half of the anteroposterior length on the non-deformed chest contour. To record accelerations of the struck-side ribcage, uniaxial accelerometers were fixed to the middle side of ribs four and eight, and the sternum.

The right-handed Cartesian coordinate system of reference was adopted. The positive x-acceleration was along the posterior-anterior direction, positive y-axis acceleration was along the left-right axis, and positive z-axis acceleration was along the superior-inferior direction. Forces followed the same sign convention. All biomechanical data were gathered according to the Society of Automotive Engineers specifications (SAE 1995). Chestband signals were filtered at class 600, and

temporal deformation contours were computed at the three locations for each test from which peak struck-side deflections and associated times of occurrences were extracted. All temporal force and deflection data were mass-scaled to 75 kg (CFR 2000; Maltese et al. 2002; Yoganandan et al. 2004). Normalized load wall forces, chest accelerations, and chest deflections were obtained by mass scaling techniques (Eppinger 1976). Following the test, specimens were palpated, a clinical-type examination for stability was performed by the clinical personnel, x-rays were obtained, and a detailed autopsy was conducted. Resulting trauma was graded based on the Abbreviated Injury Scale (AIS 1990).

RESULTS

Anthropometric data were such that the average age was 55 years, stature was 173 cm, and total body mass was 59 kg. Table 1 shows these data on a specimen-by-specimen basis. Figure 3 shows the acceleration pulse used for all tests. The mean acceleration was 13 g (standard deviation 0.1 g). A typical sled pulse is included in figure 3. The corresponding mean acceleration was 24 km/h. Peak thorax, abdomen, and pelvis forces; deflections at the upper, middle and lower levels of the chest; and upper and lower spine deflections on a test-by-test basis are included in table 2. These data are illustrated in figures 4-9. All data were scaled for the 50th percentile male body mass. For the entire test matrix, mean peak thoracic, abdominal, and pelvic forces were 4231, 4546, and 5100 N, for the 30-degree tests, and 5326, 4103, and 6729 N, for the 20-degree tests, respectively. Mean peak compressive deflections at the upper, middle and lower levels of the chest for the 30-degree tests were 96.2, 78.4, and 74.2 mm. For the 20-degree tests, these magnitudes were 75.1, 89.9, and 73.0 mm. These data are shown in figure 10. A comparison of peak chest deflections at the three levels of the chest between the current oblique experiments and previously conducted 90-degree pure lateral tests from our laboratory is shown in figure 11. Mean peak upper and lower thoracic spinous process resultant accelerations for the 30-degree and 20-degree tests were 33.3 and 46.7 g, and 67.4 and 52.0 g, respectively.

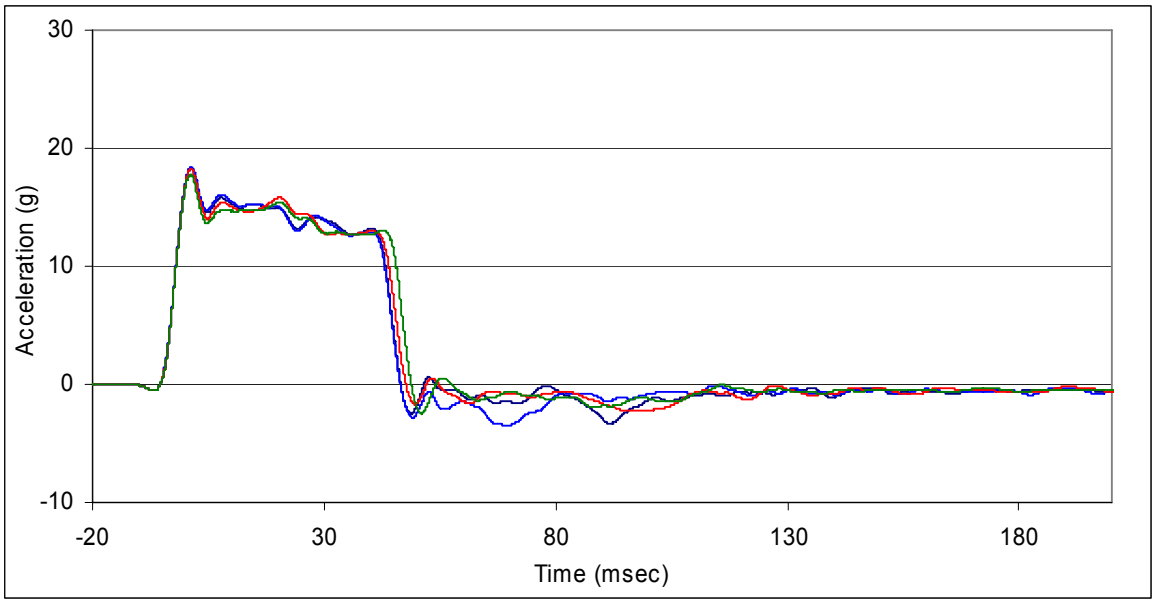

Figure 3: Acceleration profiles used for the four PMHS tests.

Table 1: PMHS data

Test Description	Age (years)	Height (m)	Weight (kg)	Skeletal injuries
30-degree PMHS test 1	56	1.72	57	Left rib 1,4,5,8 fractures and ulna fracture
30-degree PMHS test 2	74	1.50	45	Left rib 1-5, 7, 8, and right rib 5 fractures and left distal humerus fracture
20-degree PMHS test 1	43	1.82	60	Left ribs fractures 3-7, 9-10
20-degree PMHS test 2	46	1.86	73	Left rib fractures 2-6, 7-9
Mean	55	1.73	59	

Table 2: Summary of peak data

Test Description	Force (N)			Deflection (mm)			Spine Acceleration (g)	
	Thorax	Abdomen	Pelvis	Upper	Middle	Lower	Upper	Lower
20-degree PMHS 1	5,596	4,537	4,949	69.6	69.4	69.5	55.5	60.9
20-degree PMHS 2	5,057	3,669	8,509	85.3	110.4	77.6	79.3	43.1
30-degree PMHS 1	4,743	3,940	5,137	90.5	75.1	86.3	32.8	50.5
30-degree PMHS 2	3,719	5,151	5,064	101.9	81.9	67.3	33.8	41.7

DISCUSSION

As indicated, the objective of the study was to quantify forces, accelerations, and deflections, and determine chest injuries under different oblique impact vectors. A principal limitation of the study is the small sample size. Therefore, statistical analysis and corridor development were not attempted. This can be accomplished with testing of additional samples using the present protocol. From this perspective, the present results should not be generalized. However, to demonstrate the methodology, two samples each were subjected to identical lateral accelerations under two different angulations. In addition, to be consistent, data were scaled according to equal stress and equal velocity approach so that meaningful comparisons can be made between samples in the same oblique vector group and between the two groups.

As expected, variations in response characteristics were apparent between specimens, primarily due to biological variability, inherent to PMHS experimentation (Maltese et al. 2002). For example, while the peak thoracic force was very consistent in the 20-degree tests, it showed more variability in the 30-degree tests. In general, 20-degree tests resulted in greater thoracic (mean 5,326 N) and pelvic (6,729 N) forces than 30-degree tests (thorax 4,231 N, pelvis 5,100 N), while abdominal forces were greater in the 30-degree than 20-degree (4,546 N versus 4,103 N) tests. The obliqueness of the impacting vector along with individual specimen anthropometry may be responsible for these observations. In both vectors, the abdomen and thoracic plates were angled to introduce the obliqueness. However, forces in these two regions did not reach their peaks prior to forces in the pelvis region. Variations in seated height of the specimen along with changes in the distribution of the body mass and subcutaneous fat acting as a padding material, especially in the thoracic and extremity regions, might be the contributing factors. It should be noted that body mass distributions were not determined during the testing protocol and any regional alterations between specimens were not accounted for in the scaling process. In order to accommodate these factors, it is necessary to determine masses of different body regions, lower extremity, chest, etc., and suitably modify the scaling process. This is considered as an extension of the present methodology.

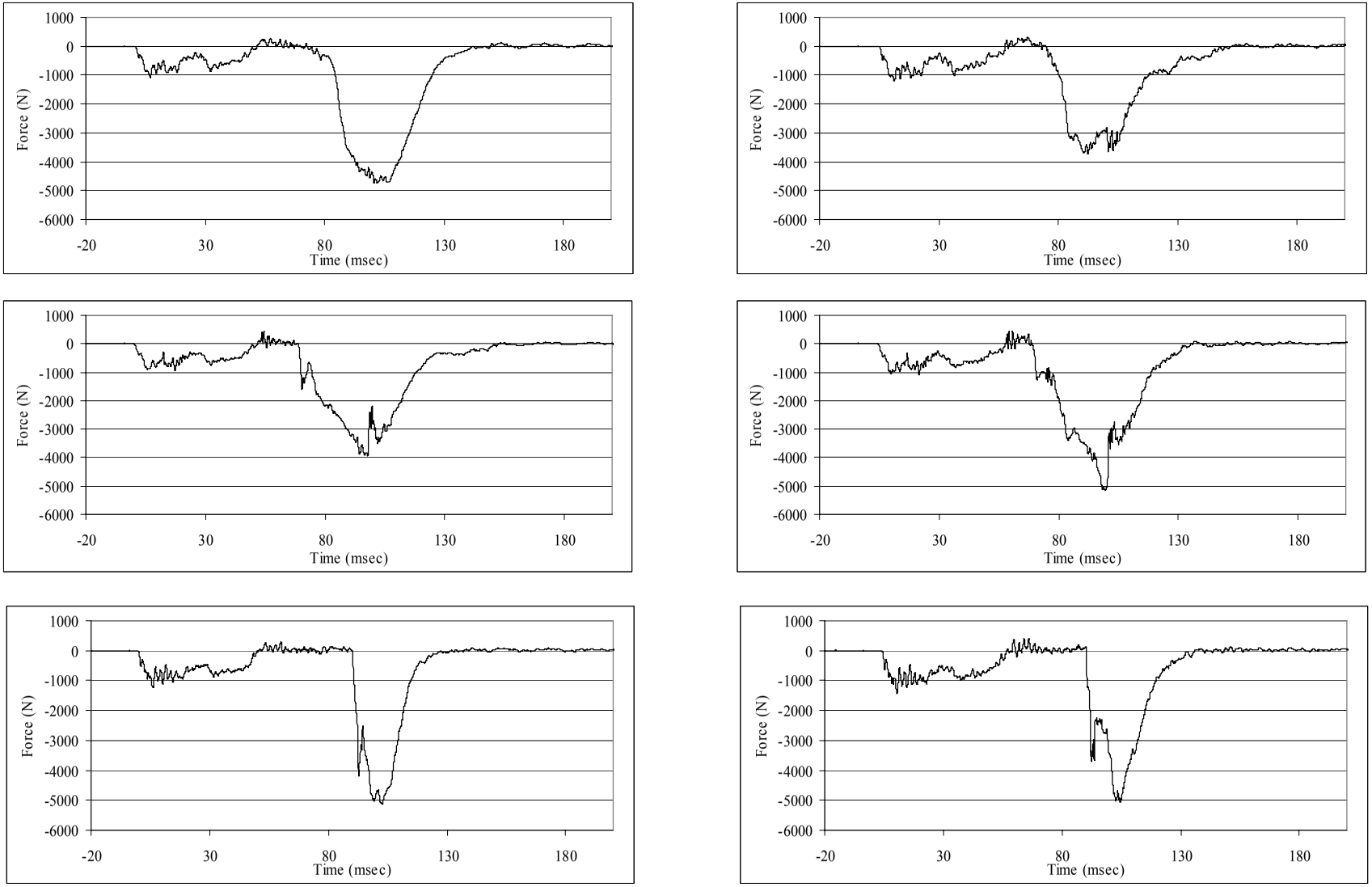

Figure 4 – Forces in the thorax (top), abdomen (middle), and pelvic (bottom) regions for 30-degree impact tests. Left column represents data from the first test and the right column represents data from the second test.

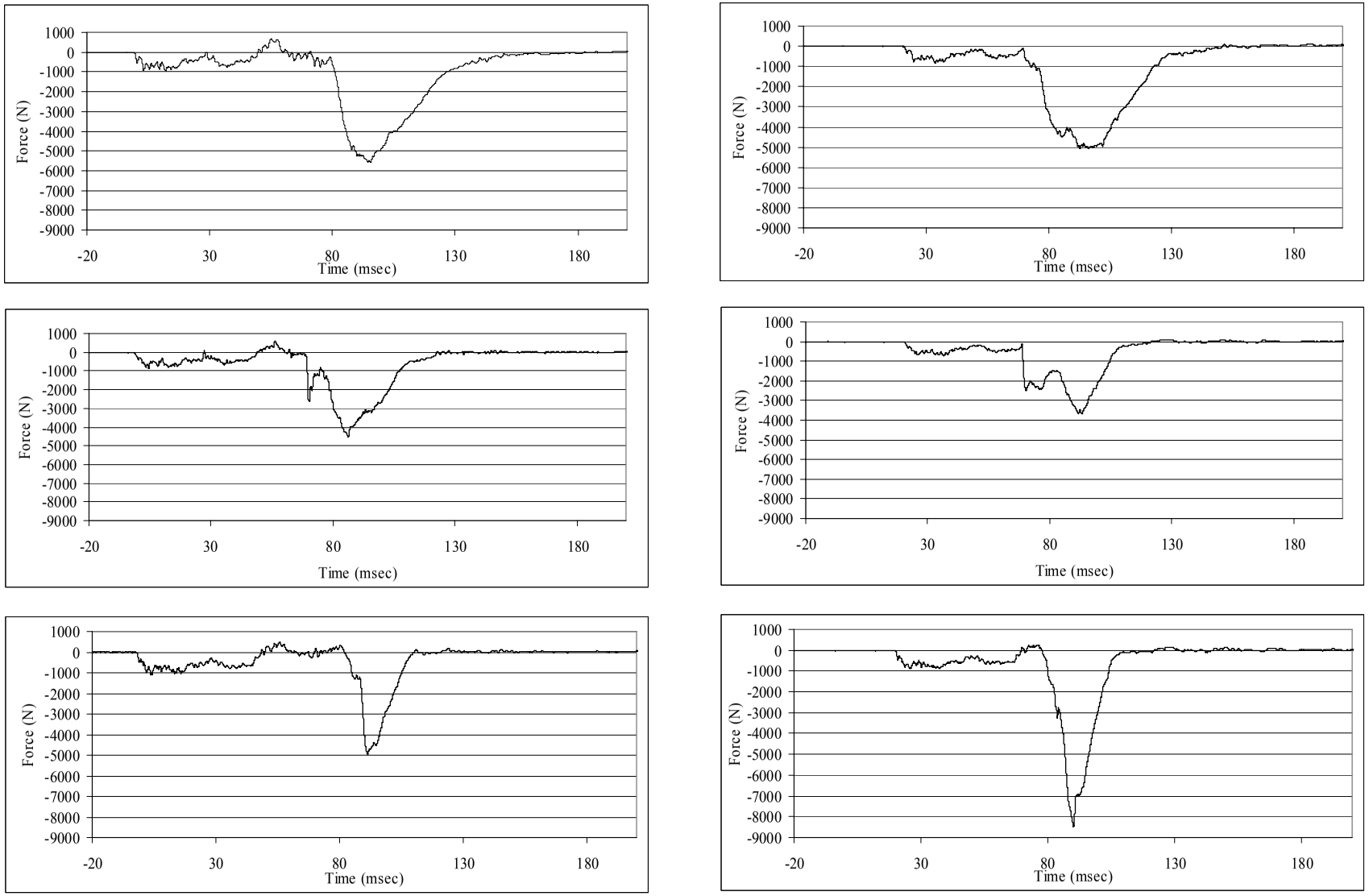

Figure 5 – Forces in the thorax (top), abdomen (middle), and pelvic (bottom) regions for 20-degree impact tests. Left column represents data from the first test and the right column represents data from the second test.

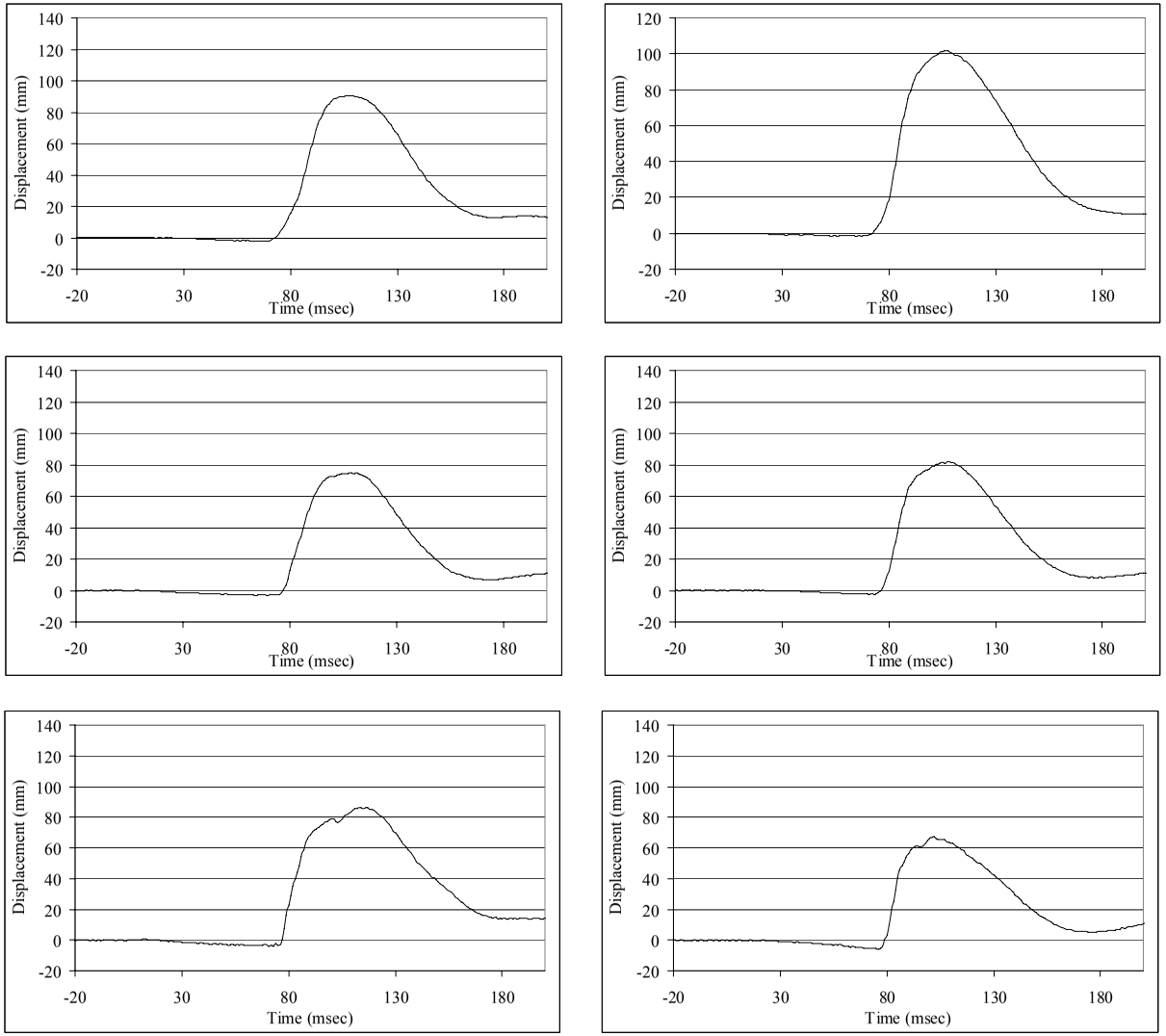

Figure 6 – Deflections derived from chestband in the upper (top), mid (middle), and lower (bottom) regions of the chest for 30-degree impact tests. Left column represents data from the first test and the right column represents data from the second test.

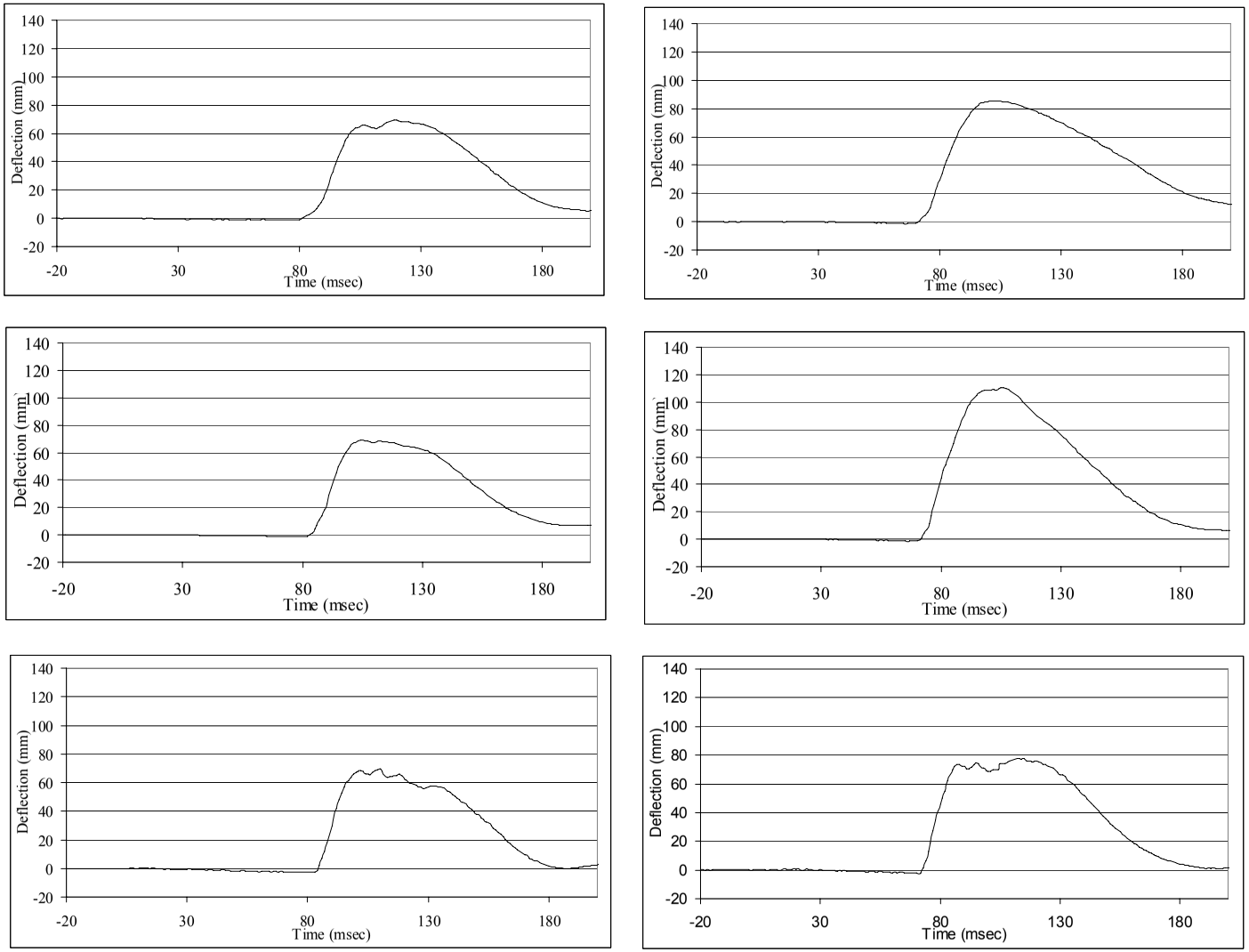

Figure 7 – Deflections from chestband in the upper (top), mid (middle), and lower (bottom) regions of the chest for 20-degree impact tests. Left column represents data from the first test and the right column represents data from the second test.

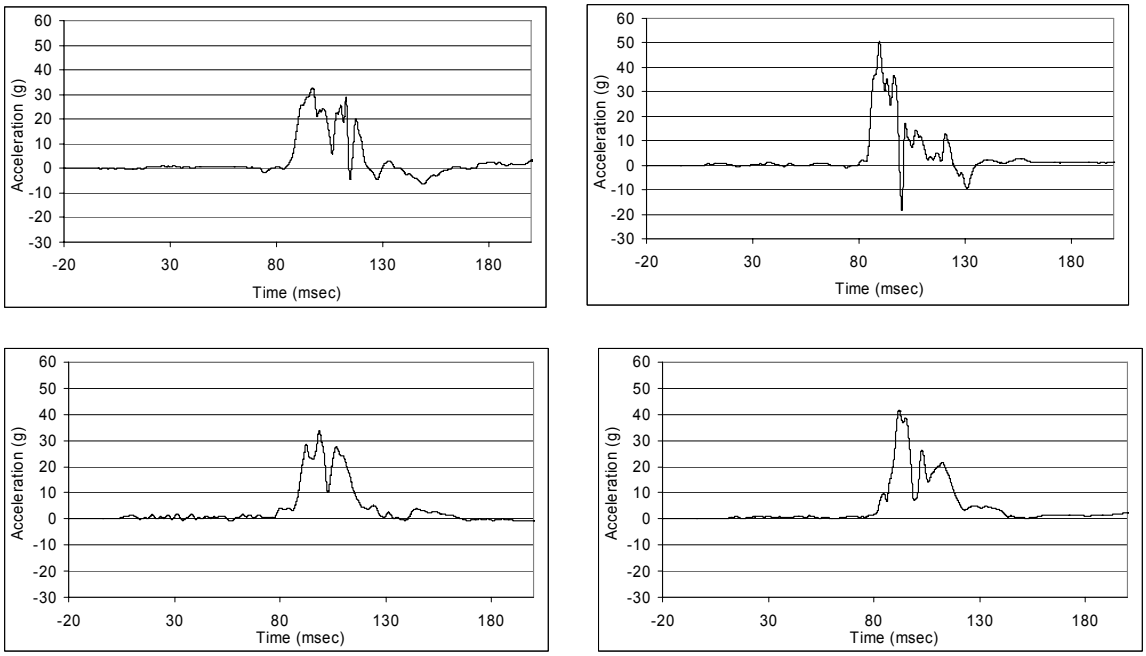

Figure 8 – Upper (top row) and lower (bottom row) spine accelerations for 30-degree tests. Left column corresponds to data from the first and the right column represents data from the second test.

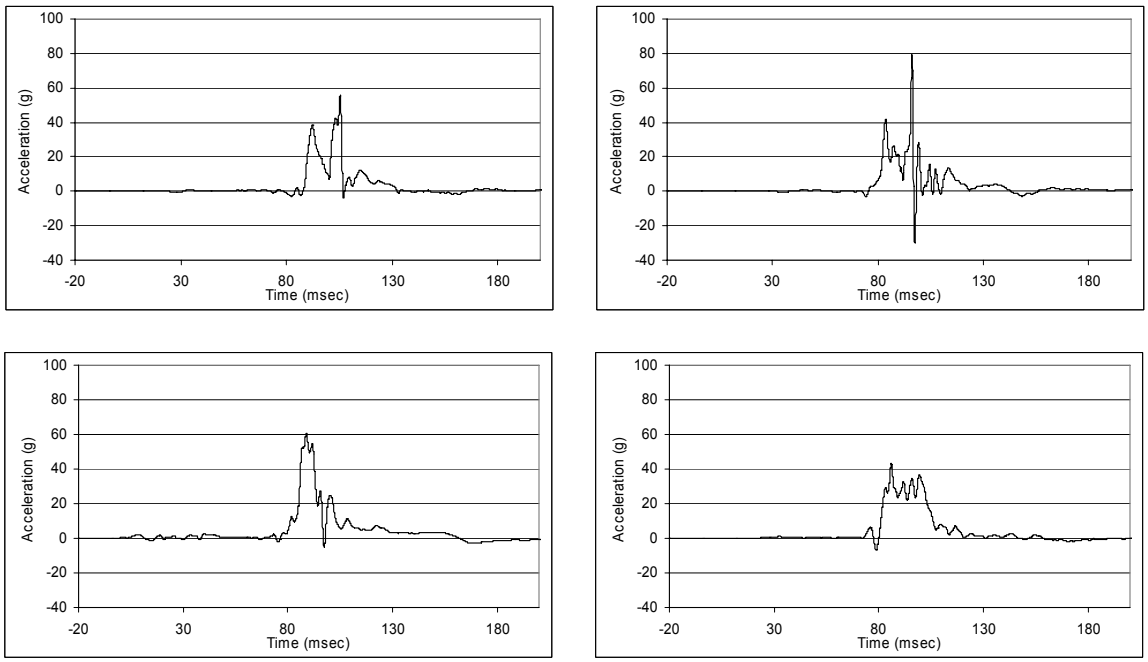

Figure 9 – Upper (top row) and lower (bottom row) spine accelerations for 20-degree tests. Left column corresponds to data from the first and the right column represents data from the second test.

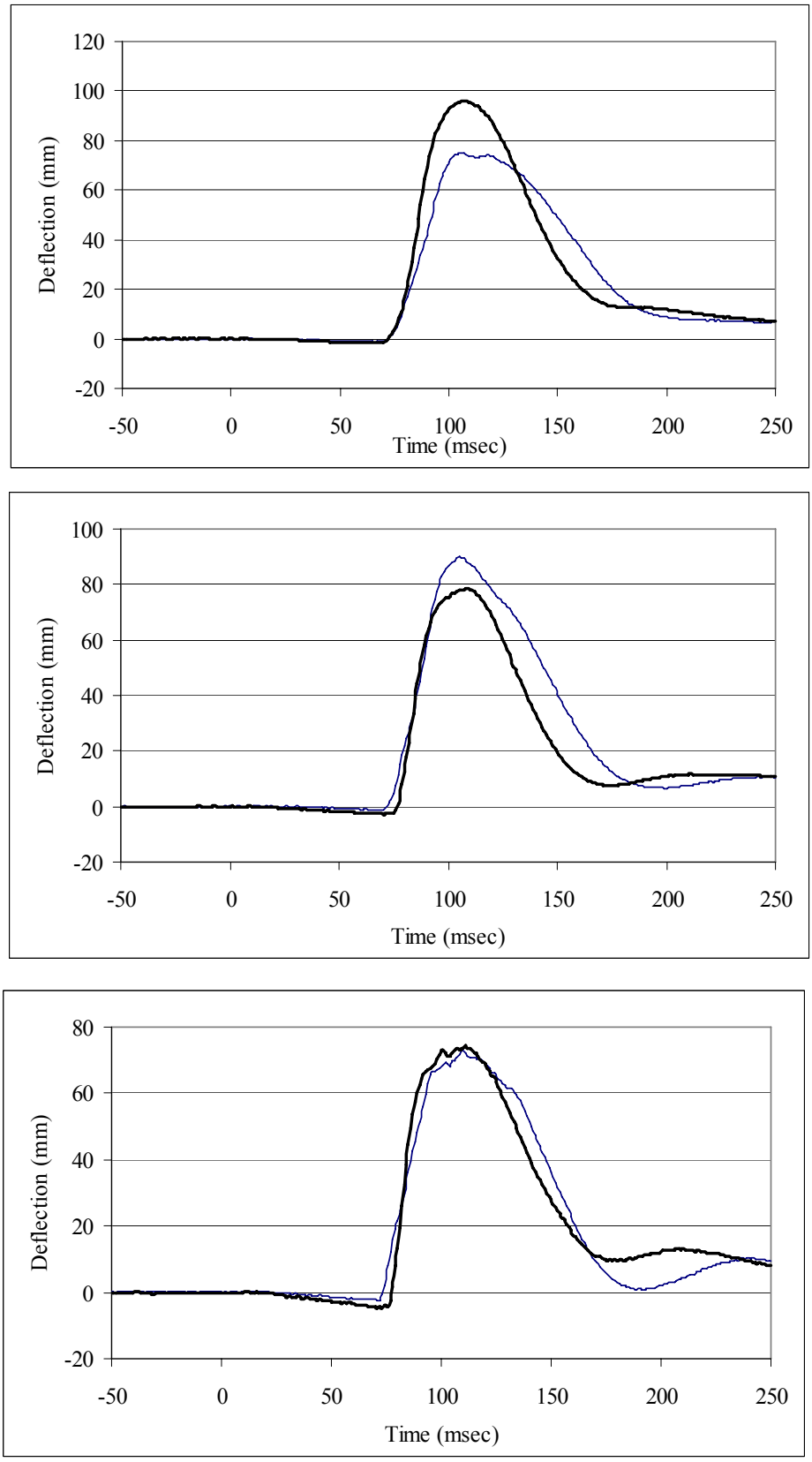

Figure 10 – Mean chest deflections in the upper (top), mid (middle) and lower (bottom row) for 20-degree (thin lines) and 30-degree (thick lines) tests.

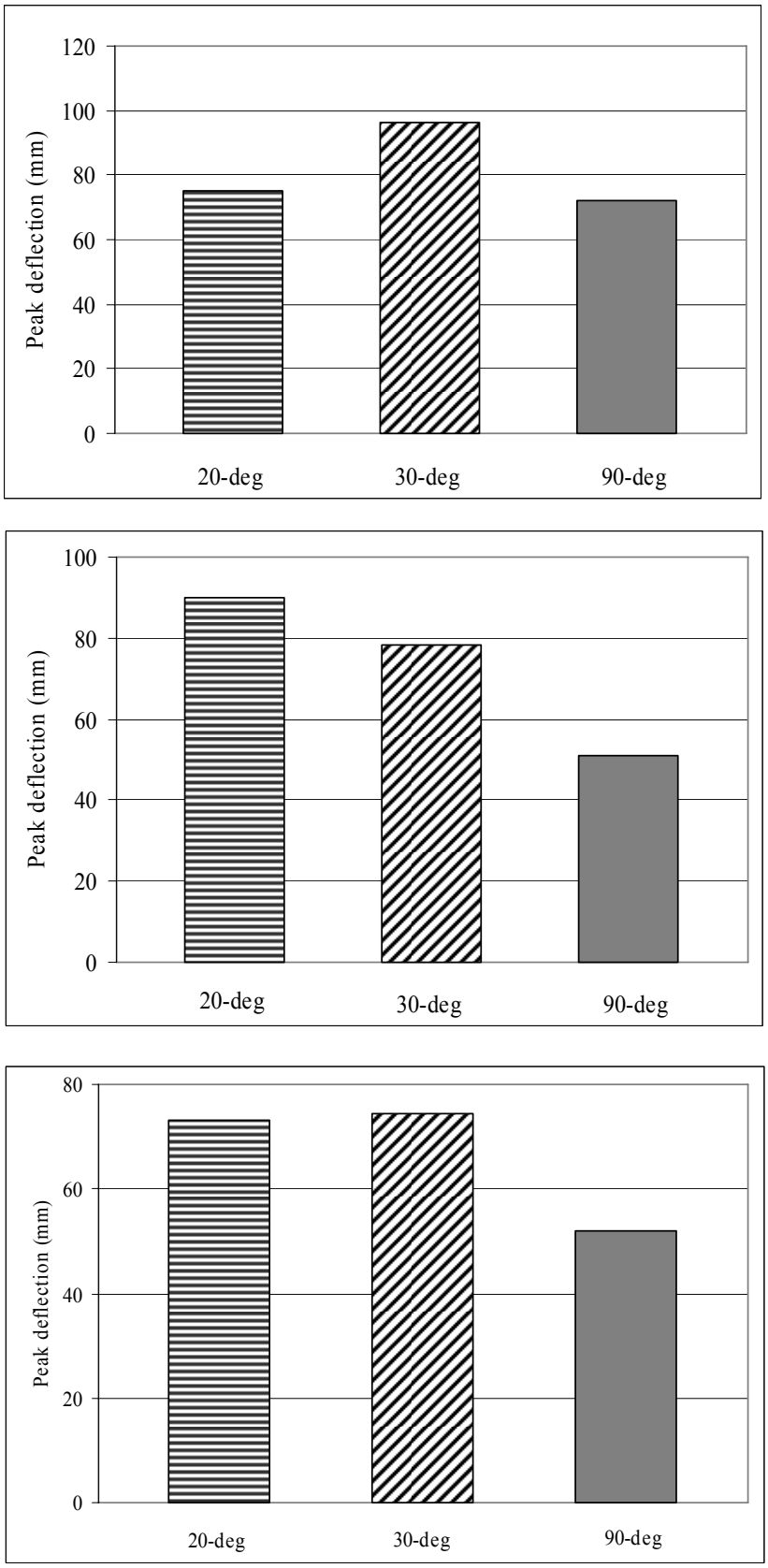

Figure 11 – Comparison of mean peak chest deflections in the upper (top), mid (middle) and lower (bottom row) for 20-, 30-, and 90-degree tests.

Contents of the human thoracic ribcage and abdomen are complex, multifunctional, three-dimensional, and from biomechanical and material property perspectives, heterogeneous. An oblique impact, at the same severity and to the same level of the chest, engages the same internal organ differently, compared to the pure lateral vector. For example, at the upper thoracic region, the pure lateral vector directly loads regions dorsal to the subclavian artery while an oblique vector at 30-degree applies impact forces to ventral arterial regions engaging the common carotid artery and brachiocephalic vein. The former vector introduces postero-anterior load transfer to these tissues, in contrast to anteroposterior load transfer by the oblique vector. The ribcage is loaded with direct compression at its most lateral region by the pure loading vector. This is in contrast to the angulated compression at the anterolateral region by the oblique vector. The anterior regions of the thoracic vertebral body sustains lateral shear in the pure loading case, whereas, it resists a force angled towards the right pedicle in the oblique case. At an inferior level, while the aorta is protected by the stomach in the pure lateral loading vector, in the oblique vector case, the major vessel is protected by the relatively smaller left lobe of the liver and its articulations (Yoganandan et al. 2000). Similar regional load transfer mechanisms are apparent as the impact vector traverses caudally. Purely anatomical considerations with respect to the impact vector in addition to functional and constitutive differences are responsible for the mechanisms of load transfer, tissue injury, and biomechanics.

The United States NCAP has an oblique force direction, 27-degree crab angle of the moving deformable barrier with respect to the stationary vehicle, and this is in contrast to the European test wherein the impact vector is perpendicular, i.e., the movable deformable barrier is at 90-degree to the stationary vehicle. The 90-degree vector induces pure lateral loading on the struck side with deformations of the ribcage initiating from the region of peak skeletal curvature. In contrast, an obliquely oriented vector induces antero-lateral compression of the ribcage on the struck side, and the impact force is thus transferred via a combined shear and compression mechanism at the initiating region. Frontal impact-induced chest injuries with belt-only versus combined airbag and belt loadings have used this type of concept for describing load transfer to skeletal structures and soft tissues and delineating injury mechanisms (Yoganandan et al. 1993; Yoganandan et al. 1996). The added shear component in the oblique side impact vector places demand on soft tissue structures housed within the ribcage. The hoop tension resulting as a consequence of the compressive deformation on the antero-lateral region superimposed with the tangential component is the primary difference in the internal load-sharing mechanism between the two modes of impact. These factors may explain the more aggressive nature of the oblique than the pure lateral vector; a finding recently observed in cases examined by CIREN; narrow object and oblique impacts imparting more severe injuries than pure side impacts (Pintar et al. 2007). This recent study reported that oblique impacts produced more unilateral fractures along with ipsilateral soft tissue trauma, a finding consistent with the present, albeit limited, dataset.

CONCLUSIONS

To understand the biomechanics of impact and injury in oblique crashes, laboratory studies were conducted with PMHS using sled equipment. Data indicated that the oblique vector results in primarily unilateral injuries to the chest, similar to field data reported in another publication by the authors of the present study. A conceptual discussion is presented comparing possible differences in the biomechanics of the human chest between pure lateral and oblique load vectors. These results, albeit from a limited sample size, will be of value in evaluating the biofidelity of anthropomorphic test devices.

ACKNOWLEDGMENTS

This research study was supported by DTNH22-03-H-07147 and VA Medical Research. The assistance of Mr. John Humm in the conduct of the test and data analysis is acknowledged.

REFERENCES

AIS. The Abbreviated Injury Scale. (1990) Arlington Heights, IL, American Association for Automotive Medicine.

CFR. Code of Federal Regulations. Washington, DC, US Department of Transportation: (2000).

ECE-R95. Uniform provisions concerning the approval of vehicles with regard to the protection of the occupants in the event of a lateral collision. (1995).

Eppinger, R. H. Prediction of thoracic injury using measurable experimental parameters. Sixth Int'l Conf on Experimental Safety Vehicles, (1976) Washington, DC, NHTSA, 770-779.

Maltese, M. R., Eppinger, R. H., Rhule, H. H., Donnelly, B. R., Pintar, F. A. and Yoganandan, N., 2002. "Response corridors of human surrogates in lateral impacts." Stapp Car Crash J 46: 321-51.

Pintar, F. A., Maiman, D. J. and Yoganandan, N. Occupant dynamics and injuries in narrow-object side impact. Experimental Safety of Vehicles, (2007) Lyon, France.

Pintar, F. A., Yoganandan, N., Hines, M. H., Maltese, M. R., McFadden, J., Saul, R., Eppinger, R., Khaewpong, N. and Kleinberger, M. Chestband analysis of human tolerance to side impact. Stapp Car Crash Conf, (1997) Lake Buena Vista, FL, 63-74.

SAE. Instrumentation for impact test-Part 1-electonic Instrumentation-SAE J211/1. Society of Automotive Engineers, Warrendale, PA: (1995).

Yoganandan, N., Morgan, R. M., Eppinger, R. H., Pintar, F. A., Sances, A., Jr. and Williams, A., 1996. "Mechanisms of thoracic injury in frontal impact." J Biomech Eng 118(4): 595-7.

Yoganandan, N., Pintar, F. A. and Gennarelli, T. Small female-specific biomechanical corridors in side impacts. IRCOBI, (2004) Graz, Austria 137-152.

Yoganandan, N., Pintar, F. A., Gennarelli, T. A. and Maltese, M. R., 2000. "Patterns of abdominal injuries in frontal and side impacts." Annu Proc Assoc Adv Automot Med 44: 17-36.

Yoganandan, N., Pintar, F. A., Skrade, D., Chmiel, W., Reinartz, J. M. and Sances, A., Jr. Thoracic biomechanics with air bag restraint. Stapp Car Crash Conf, (1993) San Antonio, TX, 133-144.

Yoganandan, N., Zhang, J., Pintar, F. A. and King Liu, Y., 2006. "Lightweight low-profile nine-accelerometer package to obtain head angular accelerations in short-duration impacts." J Biomech 39: 1347-1354.